HIGH RESOLUTION SEISMIC REFRACTION TOMOGRAPHY FOR DETERMINING DEPTH OF BLAST INDUCED DAMAGE IN A MINE WALL

J. A. Singer[1], C. A Link[2], & S. R. Iverson[3]

ABSTRACT

High resolution seismic refraction tomography has proved to be a useful tool to effectively estimate depth of blast induced damage in a mine face. Excavation blast damage can be as shallow as 1 to 2m and requires resolution at a fraction of a meter for effective imaging. We used an accelerometer with flat frequency response to 1000Hz to record data at spacings of approximately 0.25 to 0.5m along mine walls.

First arrival times from the seismic data were used to produce P-wave velocity tomograms. The tomograms show transition from low velocity zones to velocity associated with competent rock. We interpret the low velocity zones to indicate residual fracturing from blasting. Experiments on a concrete test block and at two underground mine locations give results that are consistent with fractured rock transitioning to competent rock. Our method can be applied efficiently in an underground environment to provide continuous velocity information with depth into a mine wall over a span of approximately 10m.

[1]J. A. Singer, Chevron North American Exploration and Production
[2]Address correspondence to: C. A. Link, Montana Tech, 1300 West Park St., Butte, MT, 59701, clink@mtech.edu
[3]S. R. Iverson, CDC (Centers for Disease Control)/NIOSH (National Institute for Occupational Safety and Health) SRL (Spokane Research Laboratory)

1. INTRODUCTION

Blast induced rock mass Damage (BID) is a safety concern in underground mining because it contributes to a redistribution of stresses within rock such that rock mass strength weakens from resultant blasting fractures (Raina et al. 2000). Measurement of BID can thus be a useful tool to help design and refine blasting techniques for reduced rock fracturing. Knowledge of the amount of BID can also be used to maintain safe working conditions in pre-existing tunnels and support structures by locating zones where stress has weakened rock strength over time.

High resolution seismic methods have the potential to assess the extent of BID by analyzing P-wave velocity variation with depth into the mine wall. P-waves are compressional waves observed in elastic media. The P-wave velocity generally increases with increasing consolidation of material and decreases with fracture density, thus, the fractured outer portion of a rock wall should show lower P-wave velocities than the inner undamaged rock (Kormendi et al. 1986). The method we have developed makes use of measurements on mine rock faces without the need for extra drill holes or borehole deployed equipment.

Our approach is to determine P-wave seismic velocity as a function of depth into the mine face. In zones of mostly homogeneous rock, we associate zones of low P-wave velocity with increased fracture density. We construct P-wave velocity images using seismic traveltime tomography, an inversion method for estimating P-wave velocities using first arrival times from seismic recordings. Variations of the P-wave first arrival times are used to iteratively update a grid of velocities over the surveyed area. Low velocity zones related to BID can then be identified from the tomograms (Maxwell & Young 1993).

Tomographic imaging using seismic data has been used frequently in the past few decades to study stress distribution and fracturing within rock masses. Typical seismic surveys have resolution on the order of 1m or greater and are usually large scale, covering cross-sectional areas of approximately 10,000m^2. Targets suitable for this scale are major cracks, faults, and depositional changes (Maxwell & Young 1993).

Kormendi et al. (1986) studied the correlation of rock fracturing to P-wave velocity. They used piezoelectric transducers with frequency response from 1000Hz to 2000Hz as sensors and a hammer impulse source to collect seismic transmission data. An iterative algebraic reconstruction technique was used to generate velocity maps or tomograms of surveys with dimensions 100m by 150m. Their results showed that stress conditions for a large area can be effectively monitored by seismic velocity measurements.

Maxwell and Young (1992) coupled cross-hole seismic tomography with microseismic monitoring to locate zones of anomalous stress and zones of failure in Canada's Lockerby Mine. Hydrophones with flat frequency response from 1Hz to 15 kHz were used as sensors and blasting caps were used as the seismic sources. Damped least squares inversion was used to create tomograms of the 90m by 150m survey area. Low-velocity zones were identified in the tomograms and slated for further study. The cross-hole tomography study was continued using two imaging plane depths of 6m and 10m. This method was concluded to be a useful tool for blast damage assessment.

Watanabe and Sassa (1996) used 24, single component, 40Hz natural frequency geophones to survey two sites in the Kamioka Mine in Japan. Explosives were used as impulse sources at each of the 24 geophone locations. Seismic tomography was used to analyze the first arrival data which produced images with a resolution of approximately 1m. The resulting velocity tomograms were able to clearly delineate faults.

In another study, Friedel et al. (1997) conducted a series of 3-D seismic tomographic surveys in the Lucky Friday mine near Mullan, Idaho and the Homestake mine near Lead, South Dakota. Each survey used 24, 100Hz natural frequency geophones. First arrival times were then used to produce P-wave velocity tomograms. Seismic resolution for these surveys was calculated to be approximately 7m. Seismic surveys were conducted twice for both mines to show P-wave velocity changes over a period of several months. Differences in the tomograms were attributed to rock mass failure and stope advancement.

Ashida (2001) used a tunnel boring machine as a passive source to seismically image an underground rock face. The seismic signal created by the tunnel boring machine was recorded by four three-component receivers with natural frequency of 28Hz arranged on each side of the wall at a spacing of 6m. The *x*, *y*, *z* directions of the three-component geophones were orientated to the tunnel axis directions. Twelve single-component receivers with natural frequency of 40Hz were also arranged on each side of the wall every 3m. Both arrays produced images from P-wave amplitude data that correctly identified two faults 50m and 110m from the tunnel face.

Our approach was to use available equipment (three-component accelerometer, seismic recording system) to make measurements along the mine face to be used with seismic refraction tomography to calculate P-wave velocity tomograms. We used a small hand hammer as a seismic source to tap hand placed stud bolts and were able to record seismic data with frequencies to 2000Hz. Using the first arrival times from these shot records we calculated P-wave velocity tomograms showing velocity variations 1 to 2m into the mine face that we interpreted to be associated with blast induced damage.

2. EQUIPMENT AND RECORDING PARAMETERS

High resolution seismic surveys have the potential for characterizing BID locally on very small scales. Our study uses an Applied Micro-Electro-Mechanical System (MEMS) SF3000L accelerometer as the seismic sensor. The accelerometer has a flat frequency response up to 1000Hz and is tri-axial. Output voltage for the accelerometer ranged from 0V for the horizontal axes to 1.2V for the vertical axis. The large output voltage associated with the vertical axis is due to the constant gravitational acceleration. This large output voltage prevented recording the vertical axis with our seismic recording system.

To achieve good coupling for data collection, the accelerometer was bolted to an aluminum wedge that was attached to the hand-installed stud anchor bolts. These stud anchor bolts held the accelerometer in place at survey sites and were also used as source points (Figure 1). We used a small hammer as the seismic source with an electronic trigger to send a signal to the system to begin recording when the source

was initiated. This trigger was attached to the hammer and the stud bolt to complete a simple circuit when the bolt was struck.

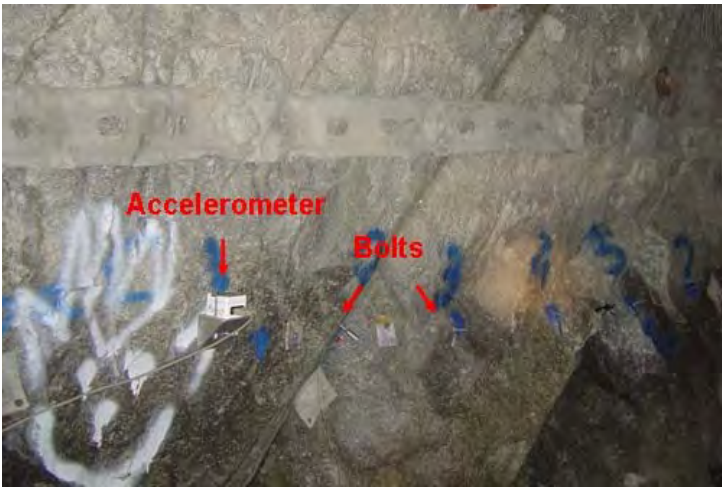

Figure 1. Photograph in the East Boulder mine showing accelerometer mounted on aluminum wedge attached to hand-installed stud bolt. The stud bolts were also used as the source points for the hammer hits.

The recording equipment consisted of a Geode seismograph (Geometrics, Inc.) and Geometrics Seismodule Controller software to store the data on a laptop computer (Figure 2). Although both horizontal axes were recorded, we only used the axis perpendicular to the mine wall for analysis. The accelerometer output for the vertical axis containing gravitational acceleration produced a signal of approximately 1.2V which was larger than the maximum allowable input voltage for the recording system. The recording sample interval for all of the surveys was 0.028033ms resulting in a Nyquist frequency of approximately 18kHz. A 60Hz notch filter was applied to all recordings to attenuate power line noise. Vertical stacking was also performed five times at each bolt station to improve the signal-to-noise ratio of the recordings by reducing random noise. Table I is a summary of the recording parameters used at all test sites.

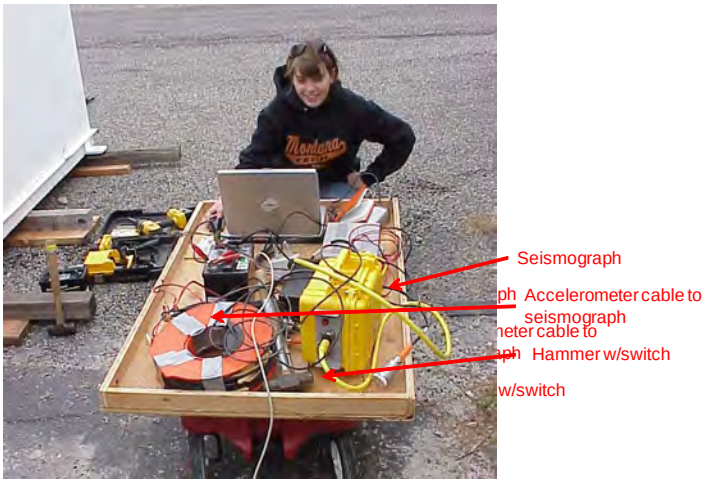

Figure 2. Photograph at the Spokane Research Laboratory concrete block test site showing the arrangement of the recording system on a coaster wagon.

Recording sample interval	28.033 μs
Nyquist frequency	17.836 kHz
Notch filter	60 Hz
Vertical stacking at each source point	5
Channels recorded	2
Receiver	3 comp. accelerometer
Source	hand-held hammer

Table I. Recording parameters for seismic recordings at all test sites.

3. DATA MANAGEMENT AND PROCESSING

3.1. Data Formatting and Preliminary Analysis

We used a reciprocal recording approach with a single receiver and multiple shot locations instead of the conventional single source and multiple receiver locations. Thus the individual shot records with the same accelerometer location were merged to create a combined file with a trace for each source location resulting in a common receiver gather. We used the Seismic Processing Workshop® (SPW/ Parallel Geosciences) Input Output Utility to combine individual files into common receiver gathers. In addition to the notch filter applied in the field, a low cut filter was applied to the data to remove low frequency noise from 0 to 10Hz.

The common receiver gather files were then reformatted for input into the seismic refraction tomography software. Figures 3a and 3b show common receiver gathers for a 20 source point survey. Figure 3a shows data prior to first arrival time picking illustrating a first arrival and the location of the accelerometer for that gather. The first arrival time picks for another gather are shown in Figure 3b and along with the picks from all gathers from the survey are then used in the refraction tomography software to calculate velocity tomograms.

Figure 4 shows a frequency power spectrum for a typical shot record from the East Boulder mine in Montana. Usable frequencies extend to approximately 2000Hz. High frequencies are important for seismic resolution as the frequencies determine the wavelength of the seismic waves through the following relationship

$$v \quad f\lambda = \tag{1}$$

where v is the seismic velocity, f is the frequency of the seismic wave and λ is the wavelength of the wave. The resulting resolution of the tomographic images is closely related to the wavelength of the seismic wave. Using a seismic velocity of 4000m/s and frequency of 2000Hz, the resulting seismic wavelength is 2m. Thus the resulting velocity images will have sub-meter resolution.

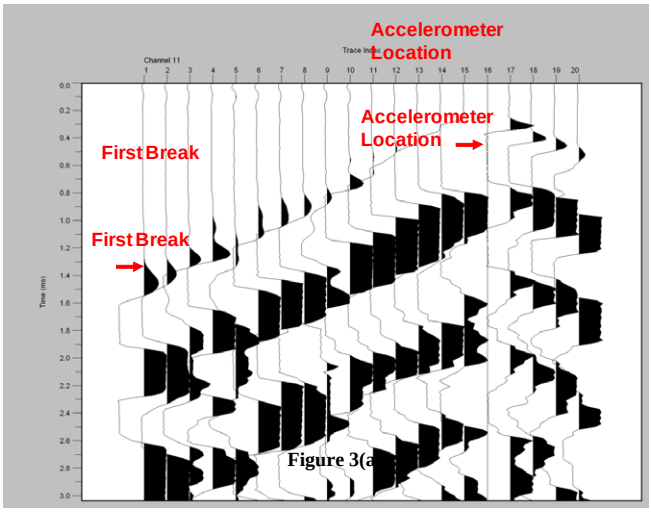

Figure 3(a)

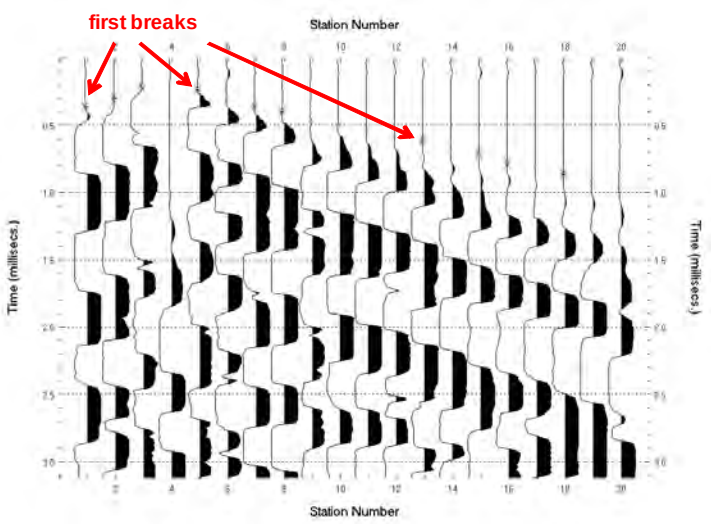

Figure 3(b)

Figure 3(a) Common receiver gather created from 20 individual source point recordings illustrating first arrival and accelerometer location. Figure 3(b) Another common receiver gather for a 20 station survey. The accelerometer position is at station 4. First arrival time picks and modeled first arrival times calculated from the resulting velocity model are shown as colored X's.

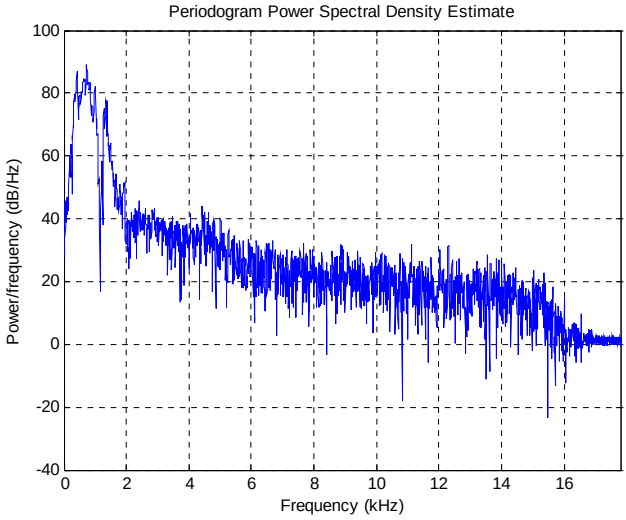

Figure 4. Frequency power spectrum for typical shot from the East Boulder mine, Montana.

The range of usable frequencies extends up to 2000Hz. These higher frequencies are necessary for resolving velocity changes at sub-meter precision.

3.2. Seismic Refraction Tomography

Seismic refraction tomography is an alternative to conventional layered seismic refraction methods. Refraction tomography performs well in many situations where conventional methods fail, for example, where there are significant lateral or vertical gradients.

There are several seismic refraction tomography software packages available. The one we used is called Rayfract® from Intelligent Resources Inc. Rayfract® images subsurface velocity using seismic first arrival energy propagation modeling. First the seismic data are imported and the 2-D profile geometry is defined, then the first arrival times are picked for all gathers (Intelligent Resources Inc. 2009). These times are used to iteratively update an initial 1-D velocity model using wave path modeling and inversion of the difference between predicted and actual travel-times.

Rayfract® uses a smooth inversion method to image velocity structure. The method is suitable for extreme topography and strong lateral velocity variation. No assignment of traces to refractors is required as in conventional layered refraction analysis. The initial 1-D velocity gradient model is determined from the first arrival travel times. This initial model is then iteratively refined using 2-D Waveform Eikonal Travel-time (WET) (Schuster and Quintus-Bosz 1993) tomographic inversion. The Fresnel volume approach is used in the inversion algorithm (Watanabe et al. 1999). This method differs from other inversion algorithms because it incorporates the fastest waveform along with waveform arrivals up to a half period slower.

Conventional ray tracing is limited to the modeling of one ray per first arrival; The WET approach models multiple signal propagation paths contributing to one first arrival. The Eikonal solver used for travel-time field computation also explicitly models diffraction in addition to refraction and transmission of seismic waves (Intelligent Resources Inc. 2009). Statistics such as the mean residual and maximum error of the fit of the modeled travel times to the measured travel times are used to quantify the goodness of fit and identify outlier time picks. Also, 2-D plots of the

wave coverage as a function of depth along the profile are calculated to help identify problematic zones or areas with low data coverage. Quality control of velocity models is also performed by direct graphical comparison of the picked first arrival times to those calculated from the model solution.

When looking at wave coverage plots, it is important to be aware that zones of low coverage, by their very nature are zones of low velocity as seismic energy follows the path of shortest time ala Fermat's principle. Conversely for high velocity zones where seismic wave paths will tend to concentrate. Thus, the coverage plots are useful for quality control purposes as well as reflecting the nature of the material through with the waves travel.

To fully take advantage of the capabilities of tomography inversion, data coverage should be high, preferably at least 7 to 8 shots per array of 24 geophones. Furthermore, the different geophone arrays should overlap by several geophone stations so as to avoid low data coverage at the boundaries (Mattsson 2007). We collected our data, albeit in the form of receiver gathers, with up to 20 shots per receiver location. Table I summarizes the number of source locations and receiver locations for each survey site.

Site	No. source locations	No. accelerometer locations	Avg. source location spacing (m)
Lucky Friday	16	5	0.4
East Boulder 1	19	6	0.5
East Boulder 2	10	5	0.6
Missile site pre-blast	20	11	0.15
Missile site post-blast	11	6	0.15

Table I. Summary of the number of source locations and the number of accelerometer locations for each of the seismic surveys.

One drawback of the WET inversion approach is the risk of velocity artifacts when using a low degree of smoothing in combination with low data coverage. This is the case especially if there are significant topography variations. We encountered some significant topography variations on the mine walls in the East Boulder mine in Montana. Another drawback is that the gradient approach used by the software may indicate increasing velocity with depth, even though the bedrock is almost homogenous rock with presumably more or less constant P-wave velocity (Mattsson 2007).

Advantages with the WET-technique are that it is fast, automated and all arrival time data are used in the creation of the velocity model. Quality control is based on statistics calculated from travel-time misfits and ray coverage plots. In the traditional refraction approach, the final velocity model is the result of a combination of manual interpolation and personal judgments made by the interpreter. This makes the traditional refraction approach less general compared with the tomographic inversion model (Mattsson 2007).

4. FOUR TEST CASES AND RESULTS

We applied our refraction tomography approach at four test sites. The first test took place at the Spokane Research Laboratory's missile test site. A concrete block had been constructed and instrumented to study the effects of a controlled blast on the material. We did seismic measurements both pre- and post-blast to determine the extent of fracturing introduced after blasting. Seismic P-wave velocity for the competent concrete in the block was approximately 3000m/s.

The second and third test sites were in the Stillwater Mining Company's East Boulder mine near Big Timber, Montana at the 6700 level. The bedrock consisted of gabbro and norite and the P-wave velocity for undamaged rock at both sites was approximately 6500m/s.

The fourth test took place in Hecla Mining Company's Lucky Friday mine at Mullan, Idaho at a depth from the surface of about 2km at the 4900 level. The rock at the test site was a phyllitic argillite with a P-wave velocity of approximately 5000m/s. Refer back to Table I for a summary of the recording geometry at each location.

4.1.1. Spokane Research Laboratory Concrete Block

4.1.1.1. Experimental setup

The first experiment involved a two-stage survey. A concrete test block was constructed by the NIOSH Spokane Research Laboratory (SRL) to be tested as part of the blasting studies in the miner safety program. The dimensions of the base of the concrete block were 3.0m by 3.0m with height 1.5m (Figure 5(a)). The block was instrumented with strain gauges to measure blast wave decay and an accelerometer to measure the acceleration of the burden as it broke free from the block. We performed our seismic refraction surveys before and after the blasting to image any changes in P-wave velocity caused by the blasting.

Survey geometry comprised 20 stations with a spacing of 0.15m. Stud anchor bolts were placed at these locations by inserting them into pre-drilled holes filled with epoxy. The bolts were placed at a height of 0.8m from the ground. Data were recorded from the accelerometer at each of the even numbered stations in the pre blasting survey. Figure 5(b) shows the survey in progress on the block. The post-blasting survey was to be a duplicate of the original survey; however, the portion of the block holding bolts 1 through 9 was destroyed (Figure 5(c)). Post-blast data were recorded with the accelerometer at even stations 10 through 20.

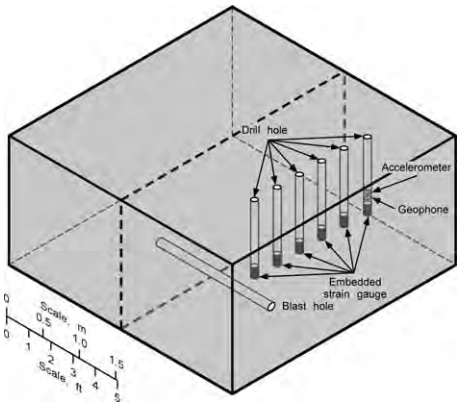

Figure 5(a)

Figure 5(b)

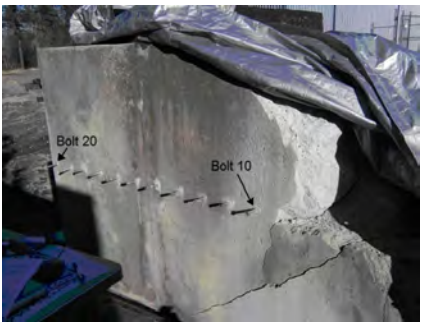

Figure 5(c)

Figure 5(a) Dimensions and some of the instrumentation on the concrete block test. The single blast hole is horizontal and was lengthened to 2.4m from 1.2m shown in the drawing. The hole was filled with Dyno AP up to 38cm from the end. Figure 5 (b) Pre-blast view of concrete test block used for blasting test. Note accelerometer and anchor bolts used for both attaching the accelerometer and as seismic source locations. Figure 5(c) Concrete test block after blasting. Rough edges and cracking are visible on the damaged end. We observed a velocity decrease of 500m/s to a depth of 0.15m between stations 10 and 12.

4.1.1.1. Results

As described in detail in section 3.2, we used Rayfract® refraction tomography software (Intelligent Resources Inc.) to generate the velocity tomograms. Rayfract® produces three outputs. The first is a 1-D velocity gradient starting model for the nonlinear inversion process, the second shows the wave coverage within the survey, and the third image is the final P-wave velocity tomogram. In the results that we show for the four test cases, we present the final velocity tomograms and the wave coverage plots.

The pre-blasting survey tomogram shows P-wave velocity quickly transitioning from low velocity at the block surface to greater than 3000m/s, the approximate velocity of competent concrete, at 1m depth (Figure 6). A velocity contour at 3000m/s is included on the tomogram for reference. The 2.85m survey imaged P-wave velocities approximately 1m into the block. The test block showed near surface oxidation from weather exposure to approximately 3cm depth. Oxidation or inconsistent curing may be the cause of the lower velocity observed from stations 912 to 920.

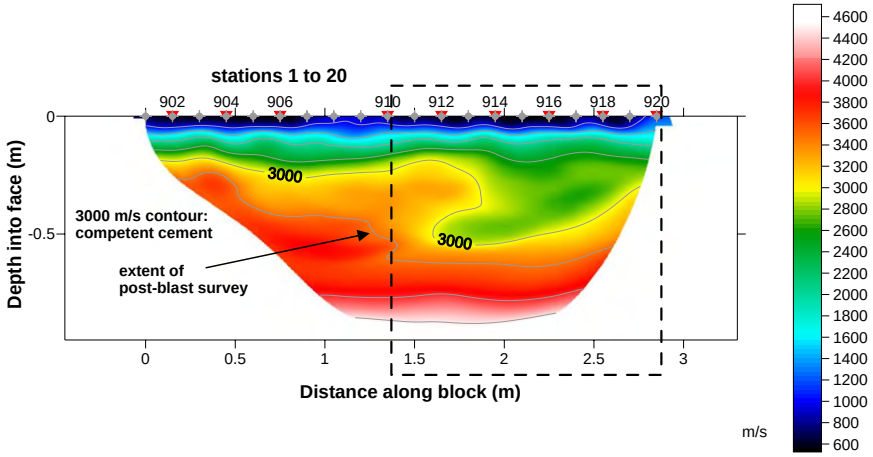

Figure 6(a)

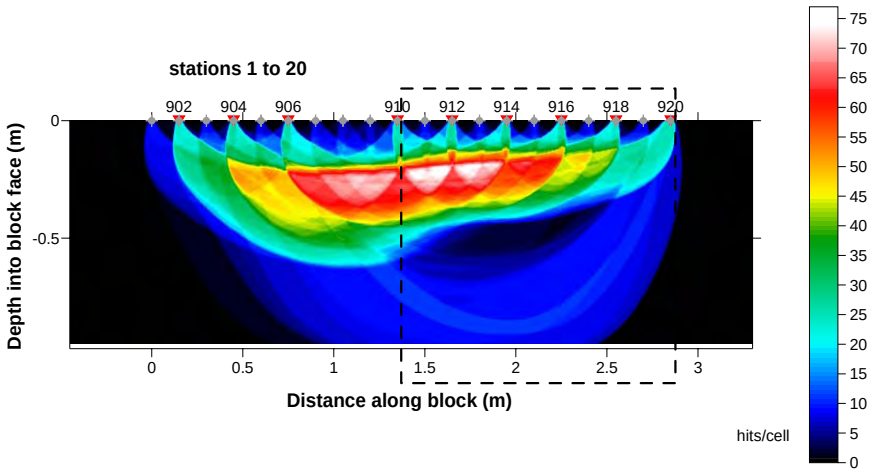

Figure 6 (b)

Figure 6 (a) Final P-wave velocity tomogram from the concrete block pre-blasting survey showing P-wave velocity quickly transitioning from a lower velocity at the block surface to greater than 3000 m/s within the block. Horizontal axis is profile distance in meters; vertical axis is depth into the block behind accelerometer positions. 9xx numbers along top represent station positions spaced 0.15m (0.5ft). Figure 6 (b) Wave coverage plot for the pre-blast survey showing even coverage through most of the imaged area. Plot dimensions are the same as for Figure 6 (a) and the color scale indicates the number of wave paths through each velocity cell or pixel.

The post-blasting survey spanned only 1.5m and P-wave velocities were imaged 0.3m into the block (Figure 7). The decrease in imaging depth is related to the decreased horizontal extent of the recording stations. Station 10 (910 in Figure 7) was located on the blasting side where velocities were expected to decrease due to the blast damage. The previous survey showed velocities between 2800 and 3000 m/s at 0.2m into the block (Figure 6). The post-blast survey shows a decrease in velocity between stations 10 and 12 at 0.2m depth. At a depth of 0.2m, station 12 shows a velocity of 2600m/s compared to 3100m/s in the pre-blast survey.

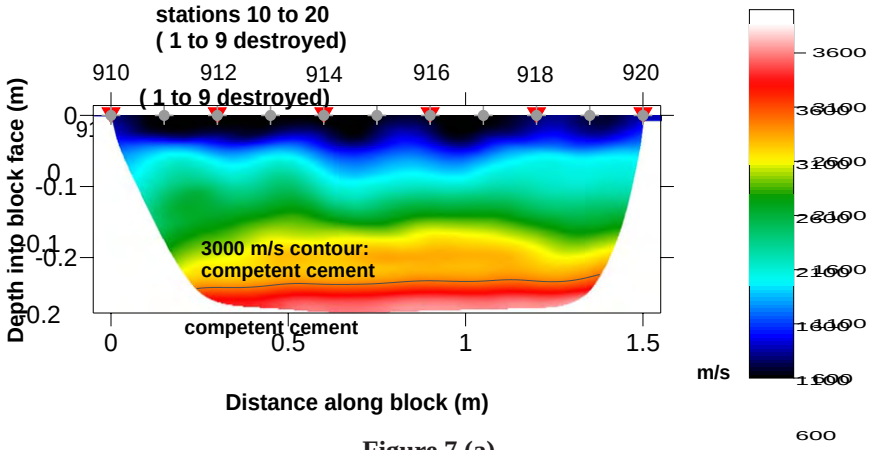

Figure 7 (a)

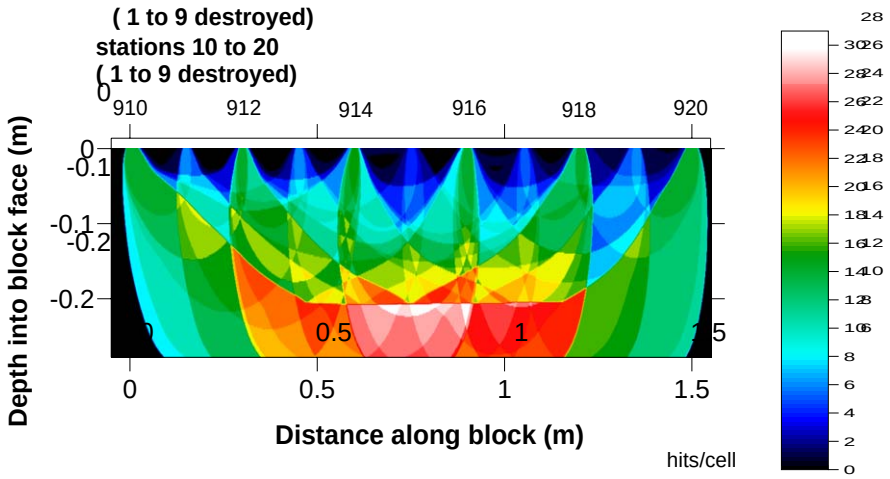

Figure 7 (b)

Figure 7 (a) Final P-wave velocity tomogram from the post blast survey showing P-wave velocity within the remaining portion of the concrete test block. Horizontal axis is profile distance in meters; vertical axis is depth into the block behind accelerometer positions. A decrease in velocity can be seen at station 910 in the post-blast survey compared to the pre-blast survey. Figure 7 (b) Wave coverage plot showing mostly even wave coverage for the portion of the block surveyed. 9xx numbers along top represent station positions spaced 0.15m (0.5ft).

To more easily identify zones of velocity change from the pre-blast to the post-blast survey, we generated a difference plot of the two tomograms (Figure 8). Both tomograms are grids of velocity values, so the pre-blasting survey was regridded and shortened to match the geometry of the post-blasting survey and subtracted from the post-blasting grid to form a difference tomogram to highlight any velocity differences. The difference tomogram shows a prominent low velocity zone that occurs between stations 10 and 12 beginning at a depth of 0.15m. The velocity in this area is approximately 500m/s lower after blasting occurred. This result was expected because the lower portion of the survey near station 10 is closest to the detonation and should have experienced the most BID. The positive velocity difference near the bottom of the difference tomogram is most likely an artifact caused by poor velocity resolution near the bottom edges of the two component tomograms resulting from the different geometries for the two surveys.

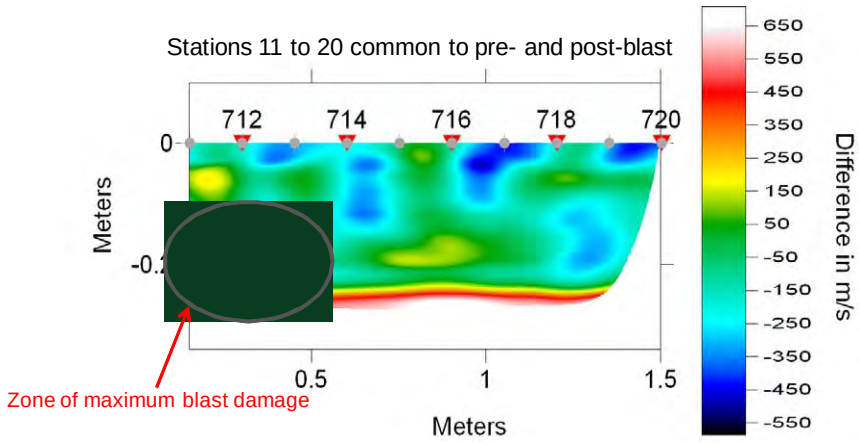

Figure 8

Figure 8. Difference tomogram of velocity images from the pre- and post-blasting surveys on the SRL concrete block. A low velocity zone at 0.2m depth is evident on the left edge of the survey and is interpreted to be a zone damaged from the blast. Horizontal axis is profile distance in meters; vertical axis is depth into the block behind accelerometer positions. 7xx numbers along top represent station positions spaced 0.15m (0.5ft).

4.1.2. Stillwater Mining Co. East Boulder Mine, Big Timber, Montana

4.1.2.1. Experimental setup

Two sites at Stillwater Mining Company's East Boulder Mine were surveyed to measure BID. The East Boulder Mine is located near Big Timber, Montana. Platinum group elements are mined underground from an ore deposit known as the J-M Reef.

We chose sites free of support bolts and mesh for the surveys. Background noise was avoided as much as possible and we tried to locate rock wall surfaces that had reasonably smooth faces for attaching the accelerometer with its recording axis perpendicular to the wall.

The first site was located on the 6700 footwall. This wall is parallel to the longitudinal orientation of the J-M Reef and was far removed from machinery noise (Figure 9). The survey length was 9.2m and 19 anchor bolt stations were installed at an approximate spacing of 0.5m. The survey area comprised gabbro between stations 1 through 8 and norite between stations 8 through 19. The uneven surface of the wall limited suitable locations for attaching the accelerometer to stations 1, 3, 14, and 16. Figure 10 is a photograph of the setup at the survey site.

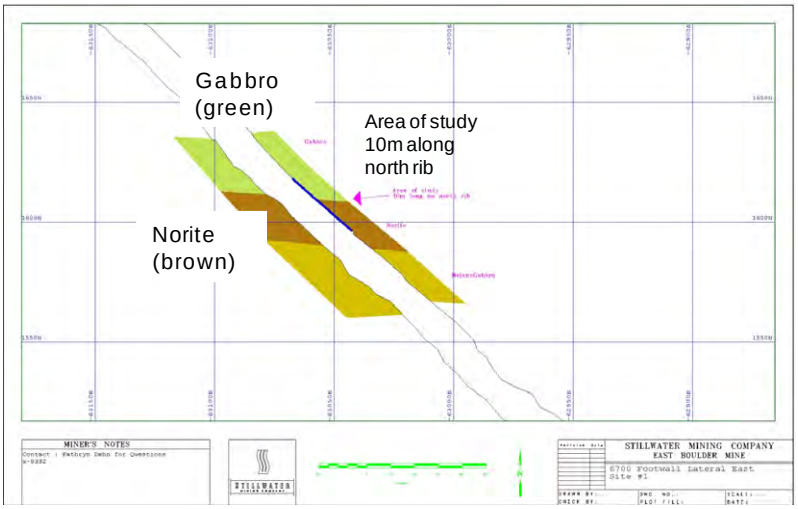

Figure 9. Schematic showing the location of the first test site at the East Boulder mine 6700 level. The study area is the blue line covering the transition from gabbro to norite.

Figure 10

Figure 10. Photograph of the first East Boulder survey site 1. The rough mine wall limited useable recording locations for the accelerometer. The bolt spacing was approximately 0.5m. Station numbers are spray painted on the mine wall above the stud bolts.

The second test site was on the 695 decline crosscut wall. This site was chosen for its perpendicular orientation to the J-M Reef longitudinal axis. Rock in this wall is composed of norite and the surface was more uneven than the first site. Figure 11 is a schematic showing the location of the survey line.

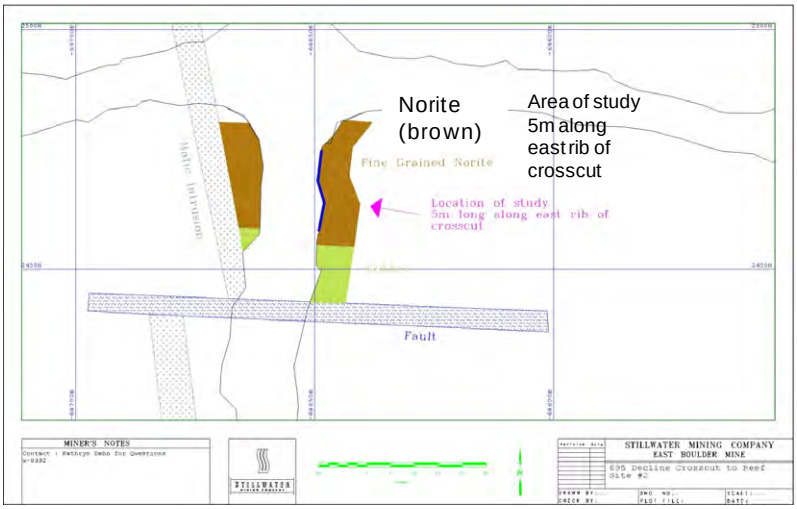

Figure 11

Figure 11. Schematic showing the location of the survey line for the second test in the East Boulder mine. The rock surveyed was norite and the surface was very uneven with mesh compounding the data acquisition.

The survey geometry for the second site consisted of 10 stations with an approximate spacing of 0.6m and the total survey length was 6.05m. The bolt positions for both sites were surveyed using a laser level and tape by referencing bolt positions on the wall to a laser line datum to give inverse wall topography. Recordings were made with the accelerometer at stations 1, 6, 7, and 9 as these were the only locations we could install the aluminum wedge to the wall for attaching the accelerometer. This site was an active working area and we tried to make our recordings during lulls in background noise caused by haul trucks.

4.1.2.2. Results

Velocity tomograms from the East Boulder Mine surveys include the wall topography of the tunnel faces. The geometry of the rock faces and the limited accelerometer recording locations for both surveys led to gaps in wave coverage. Wave coverage is an important indicator of how much confidence can be placed on calculated velocities for an area. We also increased the wave-path widths for the WET tomography in Rayfract® to improve wave coverage and provide a more robust result. For both data sets, the wave-path width was set to 0.6 % of one wave period from the default of 0.2 %.

Undamaged rock at both test sites was expected to have a P-wave velocity of approximately 6600m/s (personal communication, Kathryn Dehn). Survey site 1 results (Figure (12a)) show P-wave velocity nearing 6000m/s at the bottom of the tomogram which is interpreted to be undamaged rock. BID depth is estimated to extend 1.0m into the rock face. Wave coverage was consistent over the extent of the survey (Figure (12b)), except the shallow depths in the center where the velocity falsely appears to be less than 500m/s. We interpret the anomalously low velocity areas near the surface to be caused by lack of P-wave coverage.

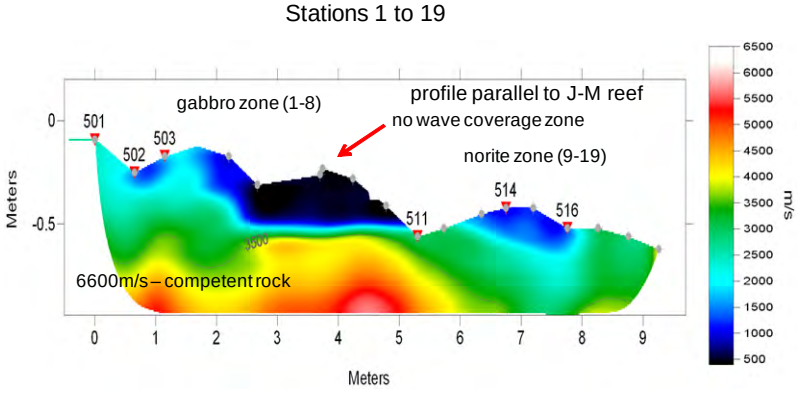

Figure 12 (a)

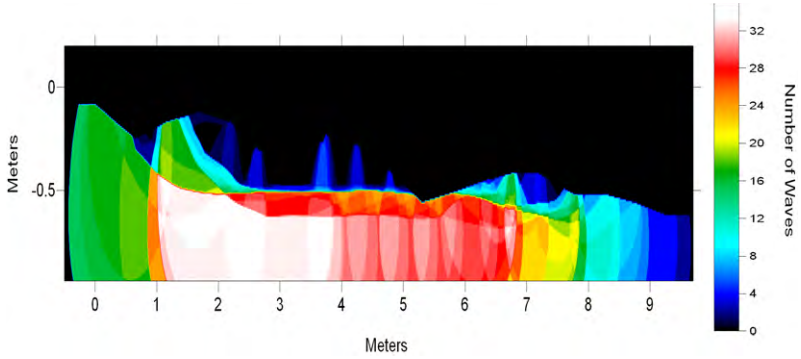

Figure 12 (b)

Figure 12(a) P-wave velocity tomogram from East Boulder site 1. Undamaged rock velocities begin at 6600 m/s. BID was estimated to a depth of 1.0m (3.3ft). Horizontal axis is profile distance in meters; vertical axis is depth into the mine wall behind accelerometer positions. 5xx numbers along top represent station positions spaced approximately 0.5m (1.6ft). Figure 12(b) Wave coverage plot for East Boulder site 1 illustrating the poor coverage in the near surface caused by the highly irregular wall topography.

The velocity tomogram for the survey at site 2 is shown in Figure 13(a). The tomogram for survey site 2 shows a maximum P-wave velocity of 4300m/s. The area between stations 1 and 3 has low wave coverage (Figure 13(b)) so velocity values there have lower confidence but are still reasonable. Velocities near station 6 are high at the surface, possibly due to the topography of the wall face or to variation in rock competence. The depth for BID was estimated to be greater than 1.5m, the maximum depth into the wall for the tomogram.

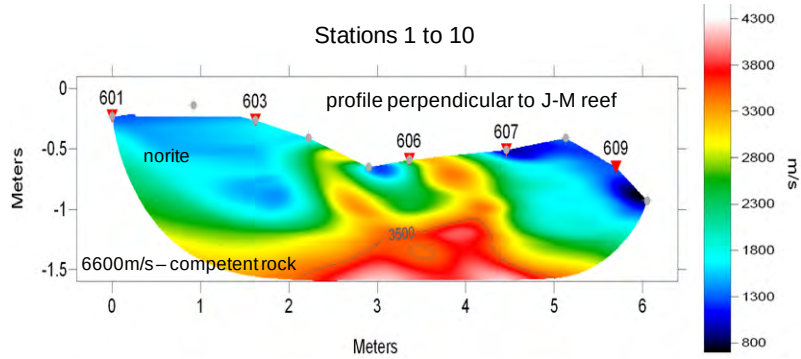

Figure 13(a)

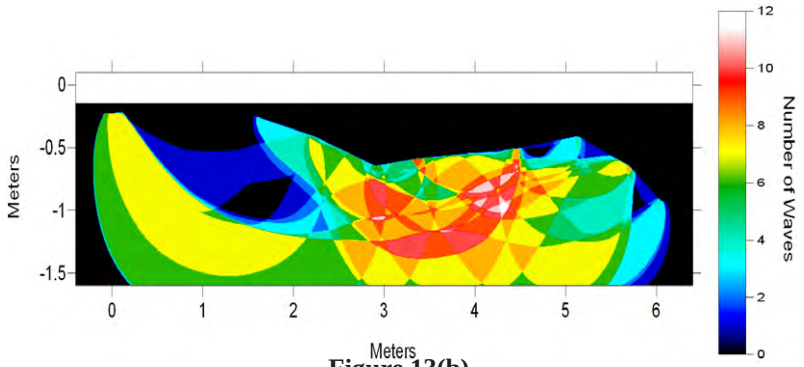

Figure 13(b)

Figure 13(a) P-wave velocity tomogram from East Boulder survey site 2 shows variable velocity layering possibly associated with rough tunnel wall or to less damaged zones of rock. Undamaged rock velocity at this site was 6600 m/s. BID was estimated to be greater than 1.5m, the maximum depth into the wall for the tomogram. Horizontal axis is profile distance in meters; vertical axis is depth into the mine wall behind accelerometer positions. 6xx numbers along top represent station positions with approximate spacing 0.6m (2.0ft). Figure 13(b) Wave coverage plot for East Boulder site 2 shows reasonable coverage for stations 603 to 608. The low velocity zone from station 601 to 603 has minimal wave path coverage.

4.1.3. Hecla Lucky Friday Mine, Mullan, Idaho

4.1.3.1. Experimental setup

The fourth seismic test was conducted at Hecla's Lucky Friday Mine in Mullan, Idaho. This mine is located in the Coeur d'Alene District and is famous for its silver rich deposits. Ore veins are located almost 2km below the surface.

Seismic recordings were made on a freshly blasted face in a 4900 level Gold Hunter vein drift. The face in this survey was considerably smoother than the excavation faces in the East Boulder Mine surveys (Figure 14). Exposed rock in the excavation was composed of phyllitic argillite with a P-wave velocity of approximately 5200m/s (personal communication, Ted Williams). The survey had 16 stations with an average spacing of 0.4m. The total length of the survey along the face was 6.6m. Recordings

were taken at accelerometer stations 3, 5, 9, 13, and 15 where good coupling could be obtained to mount the aluminum wedge for the accelerometer.

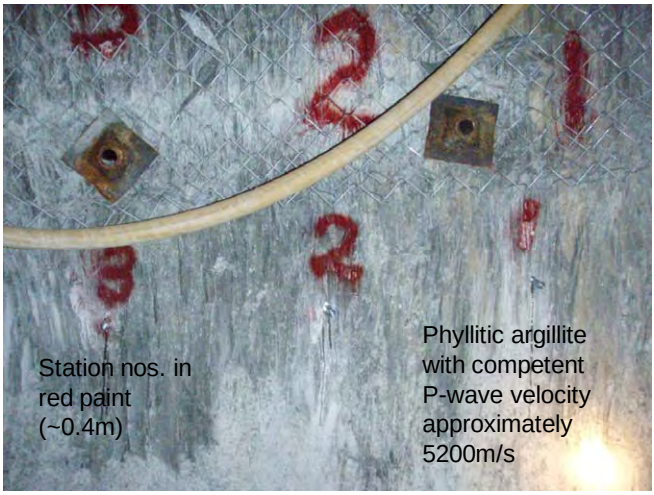

Figure 14. Photograph showing portion of rock face in the Lucky Friday mine. Spray painted numbers are above locations of epoxy mounted stud bolts.

4.1.3.2. Results

P-wave first arrivals were picked on the accelerometer recordings from stations 3, 5, 13, and 15. Station 9 recordings had high noise levels and were unusable. Lack of data at station 9 left gaps in wave coverage in the center of the survey at depths less than 0.7m (Figure 15(b)). Wave-path width in the software was again increased to 0.6 % of one wave period to smooth gaps caused by low wave coverage.

The P-wave velocity tomogram (Figure 15(a)) reaches 5200m/s, the velocity of competent rock, at approximately 1.5m into the tunnel face. The interior of the wall displays a more uniform velocity distribution than the East Boulder surveys. This could be related to the smoother mine face for the Lucky Friday survey or, conversely, the variable velocity distribution in the East Boulder surveys could be representative of the rock competence mirrored by the rough topography on the mine wall. The distribution of wave coverage (Figure 15(b)) also indicates the smoother velocity variation at the Lucky Friday site.

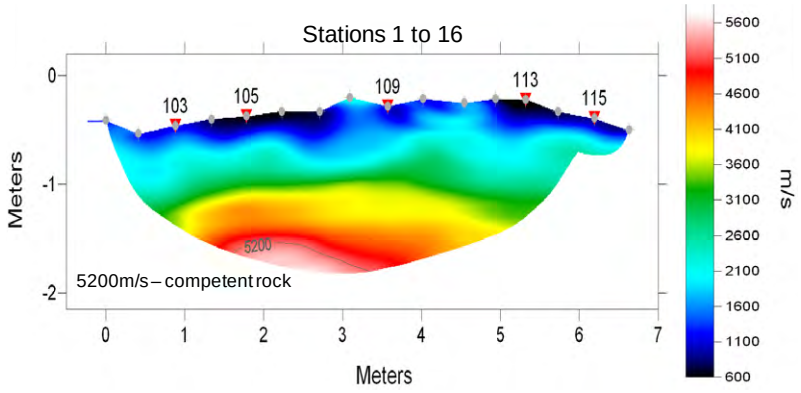

Figure 15(a)

Figure 15(a)

Figure 15(a)

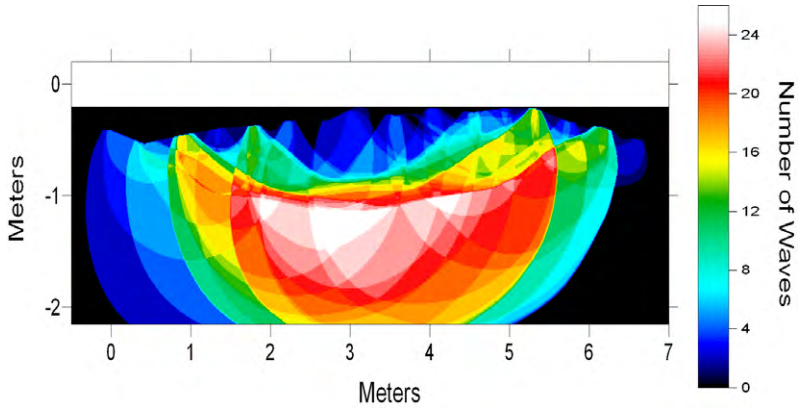

Figure 15(b)

Figure 15 (a) P-wave velocity tomogram from the Lucky Friday survey shows good rock quality beginning at about 1.5m depth. Horizontal axis is profile distance in meters; vertical axis is depth into the mine wall behind accelerometer positions. 1xx numbers along top represent station positions with approximate spacing 0.4m. (b) Wave-path coverage for the Lucky Friday survey is more even which is indicative of the smoother velocity distribution in the wall. This could be a combination of a more homogeneous nature of the rock as well as the smoother mine wall topography.

5. CONCLUSIONS

We have found that high resolution refraction tomography using a high frequency receiver can be an effective method for determining BID depth in a mine wall. A difference in P-wave velocity between concrete test block pre and post-blasting surveys was apparent on the blasted edge, with a decrease in P-wave velocity of approximately 500m/s. This velocity difference within the survey was located in the zone where blast damage was expected to have the greatest impact. The target velocity for good rock quality of 6000m/s in the East Boulder mine were found at an average depth of 1.0m at survey site 1 and 1.5m at survey site 2. A survey at the Lucky Friday mine showed good rock quality velocity of 5200m/s at approximately 1.5m depth into the wall.

A few site criteria should be considered to maximize data quality. Smoother rock faces help to improve sensor coupling and orientation for accelerometer use. Rock faces should also be mesh free if possible. Sensor recording stations should be as closely spaced as possible throughout the survey to keep wave coverage uniform at shallow depths. Survey sites should also be removed from mining activity to decrease noise in the recordings.

Although we demonstrated our approach by making surface measurements along mine wall faces using refraction tomography, we think that a better approach would be to use a borehole deployed system into the mine face. This would require purchase (or rental) of a borehole source and receiver along with recording system to record high frequencies (>5000Hz) to allow increase resolution. The advantage of the borehole system would be the ability to penetrate the boreholes to the estimated depth of competent rock and thus evenly image the space between the boreholes at high resolution. With the refraction tomography approach, the nature of the process is a decrease of wave coverage with depth. Our work was accomplished with in-house equipment and demonstrated the feasibility of the refraction approach. A higher level of resolution and accuracy could be obtained with a borehole system and a transmission tomography approach.

ACKNOWLEDGEMENTS

This study was made possible by the financial support of the National Institute of Occupational Safety and Health Order No. 212-2006-M-18282 under project director Stephen Iverson. Special thanks are extended to Ted Williams, Kathryn Dehn, Jeff Johnson, and William Hustrulid for their assistance in the seismic data collection.

REFERENCES

(1) Ashida, Y., (2001), "Seismic Imaging Ahead of a Tunnel Face with Three-component Geophones", *Int J Rock Mech and Min Sci*, 38, pp. 823-831.

(2) Friedel, M., Scott D., and Williams T., (1997), "Temporal imaging of mine-induced stress change using seismic tomography", *Engineering Geology*, 46, pp. 131-141.

(3) Håkan Mattsson, H., (2007), Interpretation of tomography inversion models for seismic refraction data along profile LFM001017 in Forsmark, in Geology – Background complementary studies Forsmark modeling stage 2.2, editors: M. B. Stephens and Kristina Skagius.

(4) Intelligent Resources Inc., (2009), http://rayfract.com.

(5) Kormendi, A., Bodoky, T., Hermann, L., Dianiska, L. and Kalman T, (1986), "Seismic Measurements for Safety in Mines", *Geophysical Prospecting*, 34, pp. 1022-1037.

(6) Maxwell, S. C. and Young, R. P, (1992), "Seismic Characterization of a Highly Stressed Rock Mass Using Tomographic Imaging and Induced Seismicity", *Journal of Geophysical Research*, 97, pp. 12361-12373.

(7) Maxwell, S. C. and Young, R. P., (1993), "Seismic Imaging of Blast Damage", *Int J Rock Mech Min Sci*, 30, pp. 1435-1440.

(8) Raina, A. K., Chakraborty, A. K., Ramulu, M. and Jethwa, J. L, (2000), "Rock mass damage from underground blasting, a literature review, and lab- and full scale tests to estimate crack depth by ultrasonic method", *Int J Blast and Frag*, 4, pp. 103-125.

(9) Schuster, G. and Quintus-Bosz, A., (1993), "Wave-path eikonal travel-time inversion: Theory", *Geophysics*, 58, pp. 1314-1323.

(10) Watanabe, T. and Sassa, K., (1996), "Seismic Attenuation Tomography and its Application to Rock Mass Evaluation", *Int J Rock Mech and Min Sci*, 33, pp. 467-477.

(11) Watanabe, T., Matsuoka, T., and Ashida, Y., (1999), "Seismic travel-time tomography using Fresnel volume approach", Expanded Abstracts 69th Anniversary International Meeting, *Society of Exploration Geophysics*, pp. 1402-1405.